

# Saturation on GEM-3

Karolina Kmiec and Francesco Renga

INFN Sezione di Roma

April 21, 2020

## 1 Measurements of saturation

The saturation effect have been studied looking at the trends of the currents on GEM-2 and GEM-3 ( $I_2$  and  $I_3$ , respectively) as a function of the high voltage applied on GEM-1 ( $HV_1$ ). Changing  $HV_1$  simulates indeed the effect on GEM-2 and GEM-3 of different energy deposits inside the chamber.

The chamber was exposed to a  $^{55}\text{Fe}$  source and the current through the  $HV_3$  bias circuit was measured. Since the bias circuit and the current readout introduce a  $25\text{ M}\Omega$  resistance in the supply line, and currents up to a few  $\mu\text{A}$  are observed in GEM-3, there can be a relevant voltage drop (up to several volts) from the power supply to the GEM. We compensated on the fly for this voltage drop by increasing the set voltage according to the drop predicted by the measured current.

The measurements of  $I_2$  and  $I_3$  have been performed alternatively, switching off the high voltage on GEM-3 ( $HV_3$ ) when the current on GEM-2 was readout, in order to not have any influence on GEM-2 from the ions going up from GEM-3 when it is on. GEM-2 is always kept at 460 V.

The measurements on GEM-3 have been always performed with a collimator in front of  $^{55}\text{Fe}$  source, in order to not have an excessive current through the  $HV_3$  bias circuit, that would have made unsafely large the necessary voltage compensation. Measurements on GEM-2 have been performed both with and without the collimator. In Fig. 1 we show the trends of  $I_2$  versus  $HV_1$ . Since the measurements without collimator are affected by large relative errors, we will use the measurements without collimator in the following, but

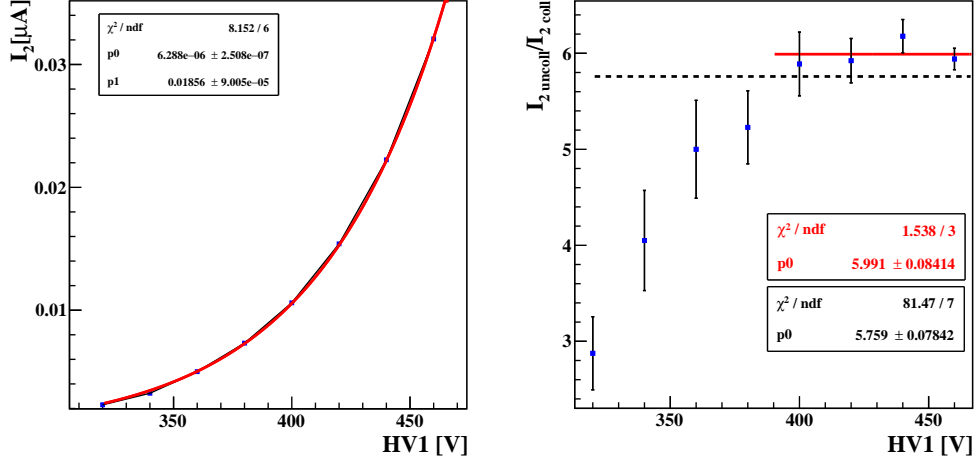


Figure 1: Measurements of  $I_2$  at various values of  $HV_1$  without (left) and with (right) a collimator in front of the  $^{55}\text{Fe}$  source. Data are fitted with and exponential function  $Ae^{-BHV_1}$ , with  $B$  in the right plot fixed to the value obtained on the left plot.

we need to scale them down to the condition with collimator in order to compare them to the measurements on GEM-3. For this purpose, an exponential fit with the function  $Ae^{-BHV_1}$  has been performed to the data without collimator, and hence to the data with collimators, fixing the parameter  $B$  from the previous fit. The ratio of the two values of  $A$ ,  $A_1/A_2 = 5.9 \pm 0.6$ , will be used to scale the values of  $I_2$  made without collimator.

We measured the current on GEM-3 for different values of  $HV_3$  and the same values on  $HV_1$  used in the measurement of  $I_2$ . In Fig. 2 we show the measurements of  $I_3$  versus the values of  $I_2$  measured at the same value of  $HV_1$  and scaled by  $A_1/A_2$ . Since  $I_2$  is proportional to the charge reaching GEM-3 from the top, and  $I_3$  is proportional to the charge produced on GEM-3, these plots show how the charge is amplified on last GEM. At  $HV_3 = 340$  V the correct linear trend is observed, showing that there is no saturation under these conditions at any value of  $HV_1$  in the considered range. At higher voltages a clear saturation trend is observed.

A different way to show the same result is in Fig. 3, where the ratio  $I_3/I_2$  is shown as a function of  $HV_1$  for different values of  $HV_3$ . Under some good

approximations, the ratio of  $I_3$  over  $I_2$  is a measurement of the gain of GEM-3. Again, the gain is constant and hence not saturated at  $HV_3 = 340$  V, while saturation is evident in the other cases<sup>1</sup>. The relative change of the gain as a function of  $I_2$  (and hence as a function of the charge reaching GEM-3), taking the gain at  $HV_1 = 340$  V as a reference, is also shown in Fig. 4.

## 2 Interpretation of the results and correction of saturation

The results of the previous section can be interpreted as follows: when an excessive reaches the same GEM hole at the same time, the gain is reduced due to the space charge shielding the electric field in the amplification region. We can try to estimate the charge necessary for the onset of this effect.

The current  $I_2$  can be written as:

$$I_2 = \Gamma N_e e G(HV_1) G(HV_2) \quad (1)$$

where  $\Gamma$  is the rate of X-ray ionization events in the chamber,  $N_e$  the number of electrons produced on average by the <sup>55</sup>Fe X-rays ( $N_e = 150$ ) from simulations with the DEGRAD software,  $e$  is the electron charge and  $G(HV)$  is the gain of any GEM in the non saturated regime at voltage  $HV$ .

In order to extract  $G(HV)$ , let us notice that the first point in each plot of Fig. 3 correspond to  $HV_1 = 340$  V,  $HV_2 = 460$  V and  $HV_3 < 460$  V. As it is usually assumed for 3-GEM stacks, these conditions are equivalent to  $HV_1 < 460$  V,  $HV_2 = 460$  V and  $HV_3 = 340$  V, and hence they correspond to non-saturated regimes. The plot of  $I_3/I_2$  as a function of  $HV_3$  with  $HV_1 = 340$  V, shown in Fig. 5 is then  $G(HV)$  in a non-saturated regime. The value of  $\Gamma$  can be then calculated from any measurement of  $I_2$ , as shown in Fig. 6. From a weighted average one gets  $\Gamma = xxx.xxx \pm xxx.xxx \text{ s}^{-1}$ .

These results also allow to translate each measurement of  $I_2$  and  $I_3$  into an average charge deposited in GEM-2 and GEM-3, that is the charges  $Q_{\text{in}}$  and  $Q_{\text{out}}$  entering and exiting GEM-3, respectively. Namely:

$$Q_{\text{in}} = N_e e G(HV_1) G(HV_2) \quad (2)$$

$$Q_{\text{out}} = \frac{I_3}{I_2} Q_{\text{in}} \quad (3)$$

---

<sup>1</sup>Notice that the presence of a non-saturated regime for GEM-3 demonstrates *a fortiori* that GEM-2 is never saturated in these measurements.

Without saturation, we would expect  $Q_{\text{out}}^{\text{exp}} = G(460 \text{ V}) Q_{\text{in}}$ . Since the effect of saturation is indeed related to the charge density, it is convenient to define the average charge densities  $\sigma_i = Q_i/\Sigma_0$ , where we choose  $\Sigma_0$  as the  $2\sigma$  area of the gaussian spots emerging from  $^{55}\text{Fe}$  under the same conditions of these measurements,  $\Sigma_0 = \pi 4\sigma^2$

In Fig. 7 we show  $\sigma_{\text{out}}^{\text{exp}}$  versus  $\sigma_{\text{out}}$ , as obtained from the measurements taken at  $HV_3 = 460 \text{ V}$  and fitted with a function that is  $\sigma_{\text{out}}^{\text{exp}} = \sigma_{\text{out}}$  below  $\sigma_0 = 4.5 \text{ pC/mm}^2$  and a second order polynomial:

$$\sigma_{\text{out}}^{\text{exp}} = a \sigma_{\text{out}}^2 + b \sigma_{\text{out}} + c \quad (4)$$

above  $\sigma_0$ , with  $b = (1 - 2a\sigma_0)$  and  $c = a\sigma_0^2$  to impose continuity of the function and its first derivative.

Although this result was obtained using the *average* densities, it can be shown analytically that, for gaussian spots and a second order polynomial curve, our choice of  $\Sigma_0$  provides the correct parameters  $a$  and  $b$  that connect the *local* charge densities.

In conclusion, if we translate the light observed in each pixel of the sCMOS camera into a charge density value, the result of Fig. 7 can be used to correct the picture *pixel by pixel* for saturation effects. Given the number of photons in a pixel,  $n_{ph}$ , we can write the charge density as:

$$\sigma = \frac{n_{ph}}{d_{px}^2} \frac{1}{\langle \frac{n_{ph}}{q} \rangle} \quad (5)$$

where  $d_{px}^2$  is the GEM area covered by one pixel ( $0.015625 \text{ mm}^2$  in LEMON) and  $\langle n_{ph}/q \rangle$  is the average number of photon produced per unit charge. We know that, on average:

$$n_{ph} = \frac{q}{e} \alpha \Omega \quad (6)$$

where  $\alpha = 0.08$  in our mixture and  $\Omega$  is the solid angle covered by the photocamera ( $\Omega = 0.00018 \text{ rad}$  in LEMON). Putting everything in Eq. (4):

$$n_{ph}^{\text{exp}} = a \left( \frac{e}{d_{px}^2 \alpha \Omega} \right) n_{ph}^2 + b n_{ph} + c \left( \frac{d_{px}^2 \alpha \Omega}{e} \right) \quad (7)$$

that is the formula to be used to correct the pixel light.

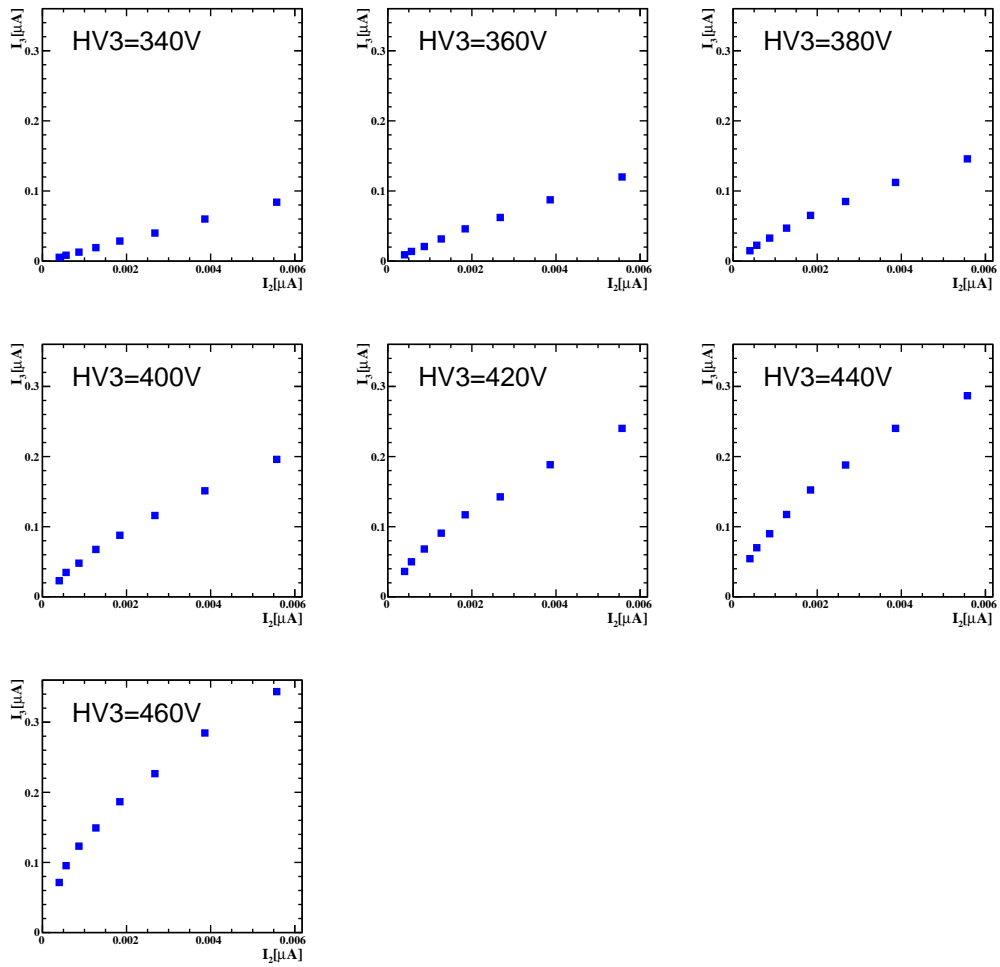


Figure 2: Measurements of  $I_3$  versus the values of  $I_2$  measured at the same value of  $HV_1$ , for different values of  $HV_3$  (from 340 V to 460 V in steps of 20 V).

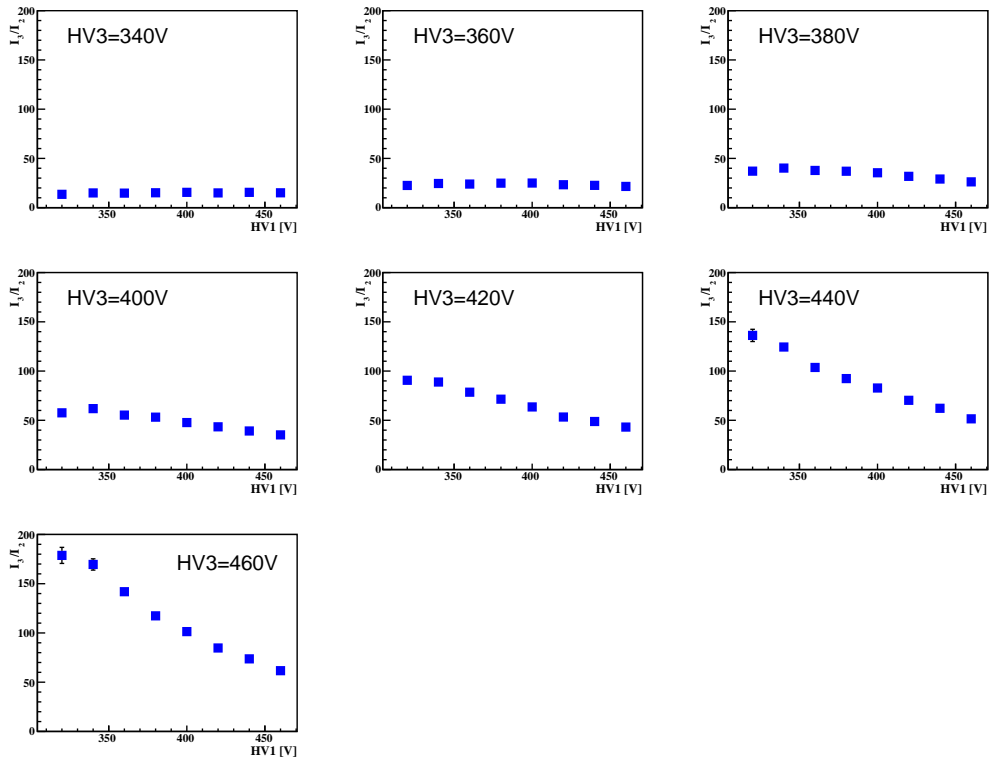


Figure 3: Measurements of  $I_3/I_2$  versus  $HV_1$ , for different values of  $HV_3$  (from 340 V to 460 V in steps of 20 V).

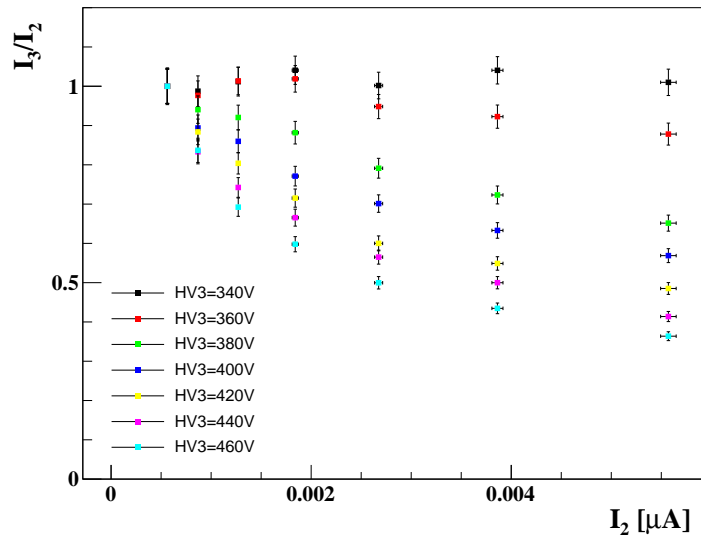


Figure 4: Measurements of  $I_3/I_2$  versus the values of  $I_2$  measured at the same value of  $HV_1$ , and normalized to the value at  $HV_1 = 340$  V, for different values of  $HV_3$ .

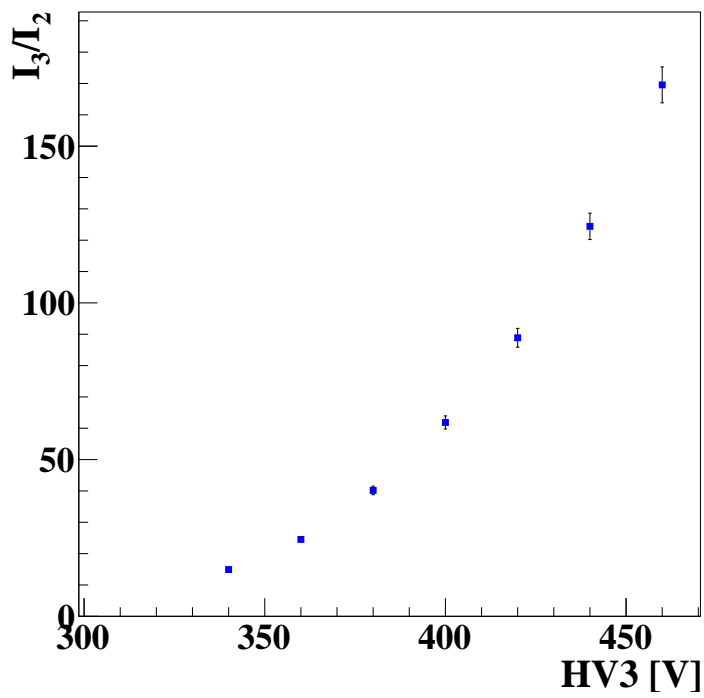


Figure 5: Measurements of  $I_3/I_2$  versus  $HV_3$  at  $HV_1 = 340$  V.



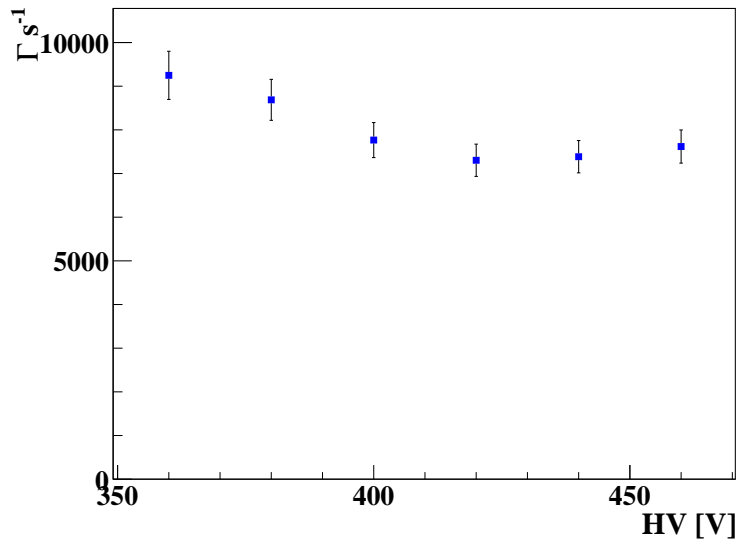


Figure 6: Value of  $\Gamma$  extracted from measurements at different values of  $HV_1$ .

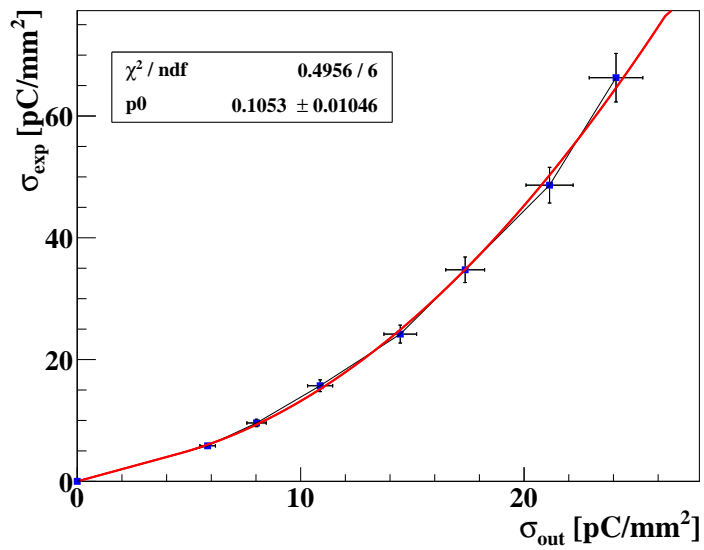


Figure 7: Expected charge density versus the measured one, at  $HV_3 = 460$  V.